Available online at www.sciencedirect.com

SciVerse ScienceDirect

Physics Procedia 32 (2012) 757 – 765

Physics Procedia

Conference Title

Microstructure and erosion resistance performance of ZrAlN/Cu coating

Jun Du[a], Xiaoying Zhu, Ping Zhang, Zhihai Cai a*

[a]*Academy of Armored Force Engineering, National Key Laboratory for Remanufacturing, Beijing 100072, China*

Abstract

ZrAlN/Cu coating has been deposited onto Ti-6Al-4V substrate by reactive magnetron sputtering in order to improve its erosion resistance. The morphology and microstructure were studied combined with Field Emission Scanning Electron Microscrope(FSEM), X-ray Diffraction(XRD), X-ray Photoelectron Spectroscopy(XPS) and Transmission Electron Microscopy(TEM). Coatings hardness and toughness were measured by nano-indentation method and Vicker indentation method respectively. It has been found that $Zr_{0.79}Al_{0.19}Cu_{0.02}N$ coating possess dense columnar structure with 20~40nm columnar grains exbibiting (100) preferential orientation. XRD reflection peaks slightly shifts to higher angle, showing some of 19at%Al and 2at%Cu substitutely dissolves into face-centered cubic(FCC) ZrN lattice, XPS proves the existence of AlN and Cu phase in coating. $Zr_{0.79}Al_{0.19}Cu_{0.02}N$ coating demonstrates best erosion resistance at 15˚~90˚ impingement angle compared with Ti6Al4V substrate, ZrN and $Zr_{0.80}Al_{0.20}N$ coating, attributing to combination of high hardness(40.7GPa) and good toughness.

Keywords: hardness; roughness; erosion resistance; magnetron sputtering

1. Introduction

Titanium alloys are known to have better mechanical properties with low density, high strength and stiffness, combined with very good creep and corrosion resistance [1]. Nowadays, Titanium alloys have been used as materials for advanced aircraft engines in the compressor section, e.g. blades and vanes, where light weight, high strength, and ductility are required [2, 3]. Airborne particles ingested by gas

* Corresponding author. Tel.: +086-010-66719249; fax: +086-010-66719249.
E-mail address: dj8378@163.com.

 doi:10.1016/j.phpro.2012.03.632

turbine engines may cause severe erosion damage to compressor gas-path components [4, 5]. This damage leads to structural and aerodynamic engine-performance deterioration [6].

Coating can enhance service life to compressor blades and vanes, and improve engine performance [7]. Although Titanium Nitride (TiN) and Zirconium Nitride (ZrN) coatings have been applied for erosion protection, the performance of coating is not completely satisfactory. It is known that alloying of TiN and ZrN coating with additional elements could introduce marked effects on coating properties and performance. For instance, it has been indicated that the addition of aluminum nitride (AlN) into TiN[8] and ZrN[9] is quite effective for high hardness and anti-oxidation character as far as these nitrides are in the form of a single phase with B1(NaCl) structure. Cu has been used to toughing ZrN[10] and TaN[11] coating., and formation of Cu network surrounding ZrN or TaN columns is expected to increase coating harness and toughness. But little work studies the combination effect when Al and Cu are added into ZrN at the same time, and there has been no research devoted to exploring erosion performance of Zr-Al-Cu-N system.

In this paper, Al and Cu (both FCC crystal structure) were added into ZrN coatings by magnetron sputtering Zr-Al-Cu alloy target in an argon/nitrogen gas mixture, the microstructure, mechanical properties and erosion resistance of coating are studied. The influence of coating hardness and toughness on erosion resistance are discussed.

2. Experimental details

The ZrN, ZrAlN and ZrAlN/Cu coatings were deposited onto Ti-6Al-4V and Si substrates by magnetron sputtering Zr, Zr-Al or Zr-Al-Cu alloy target in a mixed Ar-N_2(both with 99.999% purity) glow discharge using a N_2/Ar partial pressure of 0.4Pa and a working gas pressure of 0.3 Pa. The substrate temperature of 300˚C and the deposition time of 60 mins were kept constant for all deposition runs. The power supply was operated with a pulse frequency of 35 KHz and pulse on time of 25 μs throughout the entire deposition cycle.

The coatings were deposited under the following conditions: discharge voltage=400 V, discharge current=3 A, substrate-to-target distance=180 mm, substrate biases ranging from the floating potential to -110 V, duty cycle is 40%.

The microstructure, phase and chemical composition of coatings were analyzed using a combination of XRD with Cu-Kα radiation in the 2θ range 20~80˚, FESEM-EDS, XPS and TEM. XPS was used to provide general information on chemical bonding, it was undertaken using monochromatic Al Kα radiation(1486.6 eV). The binding energies were referenced to the C1s peak (285.0 eV). The nanohardness and elastic modulus were determined from indentation loading/unloading curves generated with a Berkovich indenter using Oliver-Pharr method. A maximum load of 10 mN was applied, which corresponded to maximum indentation depths of less than 10% of the coating thickness, to minimize the substrate influence on the measurement. Quantitatively, coatings fracture toughness(K_{IC}) were calculated through, $K_{IC} = \delta\left(E/H\right)^{1/2}\left(P/c^{3/2}\right)$where P is the applied indentation load, E and H are the elastic modulus and hardness of the film, respectively. δ is emperical constant, for standard Vikers cube cornor indenter, taken as 0.0319[12], c is crack length which can be obtained using SEM[13]. Erosion tests were performed using silicon carbide powders with an average size of 80 μm. The particle-N_2 gas steam was directed towards the testing coupon at impingement angles of 15˚, 30˚, 45˚, 60˚ and 90˚. A particle velocity of 60 m/s, and an average particle feed rate of 1~2g/min were used in each test. The weight loss of the tested coupon was measured using a balance with an accuracy of 10^{-5} g.

3. Results and discussion

3.1. Crystalline Structure

The chemical composition of ZrAlN and ZrAlN/Cu coating is $Zr_{0.80}Al_{0.20}N$ and $Zr_{0.79}Al_{0.19}Cu_{0.02}N$ (a.u.). Fig.1 illustrates the cross-sectional FESEM image of ZrAlN/Cu coating which can be divided into three layers, namely bonding layer, transition layer and ceramics supporting layer. Metal Zr was magnetron sputtering onto substrate firstly in order to improve bonding strength between coating and substrate (bonding layer), then nitrogen gas was gradually charged into chamber to reduce internal stress (transition layer), finally magnetron sputtering Zr-Al-Cu to form ceramics supporting layer. Fig.1 shows that coating of such composition possess fully dense morphology and a reasonably flat surface. This kind of structure is usually ascribed to the 'high temperature' (Zone II) region of the commonly accepted structure zone models (SZM) [14]. Since Cu has a relatively low melting temperature T_m (1356 K) and a high homologous temperature T_s/T_m (≈0.3), while the equivalent values for ZrN are 3233 K and 0.12, respectively, hence Cu-containing coatings should exhibit dense morphology. The coating thickness is about 1.4 μm.

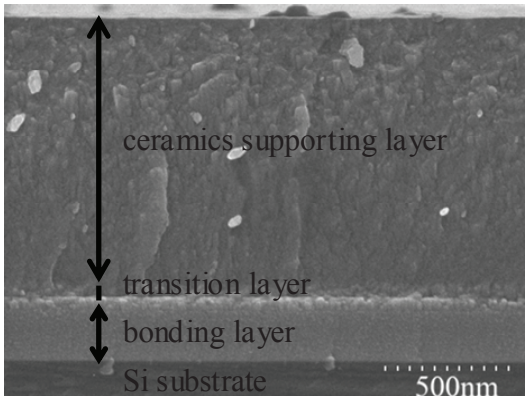

Fig.1 The cross-sectional morphology of multicomponent ZrAlN/Cu coating

An XRD pattern of $Zr_{0.79}Al_{0.19}Cu_{0.02}N$ deposited onto Ti alloy substrate is shown in Fig.2. The spectrum exhibits the (200), (220) ZrN reflections and (101), (002) and (100) Ti reflections, this coating shows ZrN(100) preferential orientation which could be easily understood by comparing XRD pattern with standand diffraction spetrum given below in Fig.2. Because ZrN coating can easily take B1 lattice, it is usually suggested that the XRD peak near 2θ=32˚ is attributed to B1 structure. However, the XRD peak near 2θ=32˚ in Fig.2 is not simply assigned with ZrN B1 structure because the peak is broad and the position slightly shifted to higher angles, implying formation of wurtzite AlN(w-AlN) phase in addition to the B1 structured solid solution(Zr,Al)N phase. In Zr-Al-N system, the decrease of lattice constant is easily determined with the presence of AlN [9]. This implies significant dissolution of Al or Cu in ZrN and substitution of Zr by smaller Al or Cu atoms, consequently modified coatings lattice parameter.

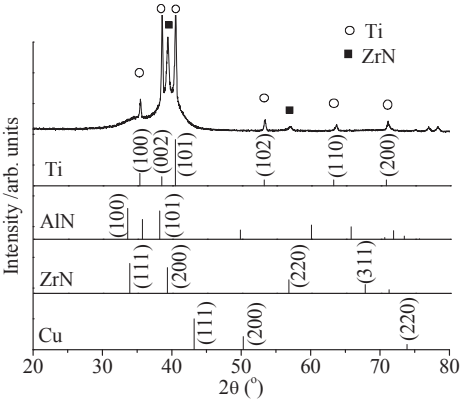

Fig.2 XRD of ZrAlN/Cu coating on titanium alloy substrate

Fig.3 shows the cross-sectional bright-field (BF) TEM micrograph of ZrAlN/Cu coating. Coating can be divided into three layers, from right to left are the (I) bonding layer, (II) transition layer and (III) ZrAlN/Cu layer. It must be pointed out that three layers show different structural characteristics. There is no significant structural feature for bonding layer; no columnar grain can be detected. While transition layer and ZrAlN/Cu layer possess dense, columnar structure (such as that seen for many other transition metal nitride coatings). It is evident from this figure that the columns are in the approximate range 20~40 nm and perpendicular to coating/substrate interface. No morphology defects were detected. Selected-area electron diffraction(SAED) pattern suggests that the coating is a polycrystalline material with grains almost randomly oriented. However, the fact that the rings are not completely continuous suggests the presence of a certain amount of texture in the coating. In this case, more of the crystals occur with a specific orientation than would occur randomly.

Detailed XPS narrow spectra of Zr3d, Cu2p, Al2p and N1s peaks for ZrAlN/Cu coating are shown in Figure 4. From the spectrum deconvolution of Zr3d doublet(Fig.4a), two characteristic lines appear which are assigned to Zr-N and Zr-O bonds. For the case of Zr-N bond, binding energies could be indentified Zr3d5/2 at 179.9eV and Zr3d3/2 at 182.33eV, as for the Zr-O bond, Zr3d5/2 at 182.16eV. From the spectrum of Cu2p(Fig.4b), these two peaks could be indentified Cu2p3 at 932.6eV and Cu2p1 at 952.2eV. Relating XRD to XPS, Cu is expected distribute as disperse phase with nano crystalline in ZrAlN/Cu coating rather than react with Zr, Al and N. The deconvolution of the spectrum of Al2p doublet is shown in Fig.4c, peaks are decomposed in two characteristic lines, which are assigned to Al-N at 73.8eV and Al-O at 76.6eV. From the spectrum deconvolution of N1s, which is shown in Fig.4d, this peak becomes in two lines, the higher energy line is assigned to Zr-N bond with a binding energy of 397.7eV, the lower

energy line is assigned to Al-N bond with a binding energy of 395.6eV. The formation of AlN is clarified by XPS results.

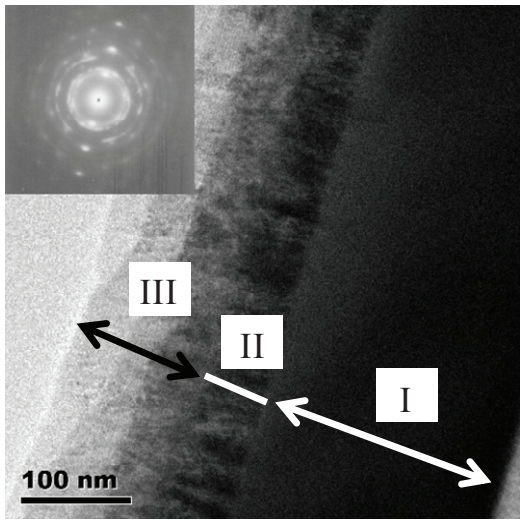

Fig.3 TEM of ZrAlN/Cu coating

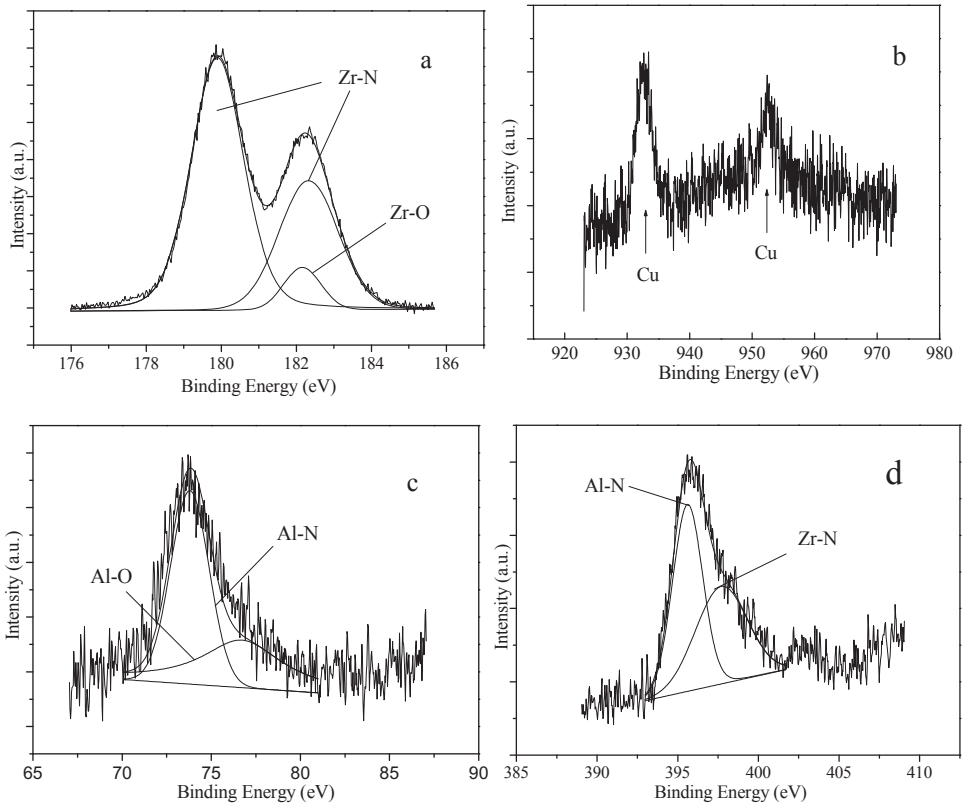

Fig.4 XPS spectrum of ZrAlN/Cu coating a) Zr3d b)Cu2p c)Al2p d)N1s

3.2. Hardness and toughness

The microhardness(H), Young's modulus(E^*) and elastic recovery(W_e) are basic quantities characterizing mechanical behavior of nano-scale coatings. Measured values of H and E^* enable to calculate the ratio H^3/E^{*2}, which gives the information on a resistance of materials to plastic deformation[15]. The resistance to plastic deformation increases with increasing ratio H^3/E^{*2}. It has been found that coating toughness increase with increasing H^3/E^{*2}, a low E is desirable because it allows a given load to be distributed over a wider area[16].

Fig.5 is nanoidentation load-unload curves of multicomponent ZrAlN/Cu coating. Hardness and elastic modulus can been drawn from this figure as 40.7 GPa and 257.8 GPa respectively. Coating ZrN and ZrAlN hardness are also obtained using this method, as are shown in Table.1.

ZrAlN($Zr_{0.80}Al_{0.20}N$) possess hardness value 2 times than ZrN, the hardness enhancement has been partly attributed to Al incorporation introducing solid solution harden effect[17]. Hardness of ZrAlN/Cu($Zr_{0.79}Al_{0.19}Cu_{0.02}N$) is higher than that of ZrAlN a little bit, whereas elastic modulus of ZrAlN/Cu is lower, so higher value of H^3/E^{*2} is achieved, that means ZrAlN/Cu has better resistance to plastic deformation, or more tougher. The effect of Cu on coating hardness is still in debate, some papers have reported soft Cu increases hardness of ZrCuN coating[18], whereas some others believe Cu decrease hardness[19]. In this paper, as far as $Zr_{0.79}Al_{0.19}Cu_{0.02}N$ is concerned, 2at%Cu doesn't decrease hardness.

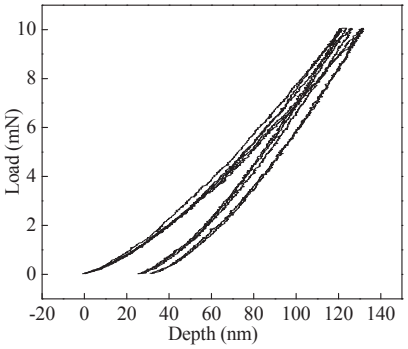

Fig.5 The loading/unloading curves of ZrAlN/Cu coating

It is very difficult to adequately measure the toughness of a thin coating. At present, there is neither standard test procedure nor standard methodology for accessment of toughness of thin films, Perhaps indentation is the most widely used tool in assessment of thin film toughness[20]. Table.1 shows the K_{IC} of coating ZrN, ZrAlN and ZrAlN/Cu obtained using indentation mothed. ZrAlN/Cu has the highest K_{IC} as well as hardness, that means this coating is more tougher than ZrN and ZrAlN. Relating hardness to toughness, ductile phase Cu favors mechanical properties of coating ZrAlN/Cu, it overcomes the brittleness of ZrAlN, enhances coating toughness. As a ductile phase in coating, two mechanisms are responsible for the enhanced toughness: First, relaxation of the strain field around the crack tip through deformation or crack blunting, whereby the work for plastic deformation is increased. Second, bridging of cracks by ligaments of the ductile phase behind the advancing crack tip. The enhanced toughness of high hardness ZrAlN/Cu coating favours the erosion resistance as follows.

3.3. Erosion resistance

It is well known that particle velocity, particle impingement angle, particle characteristics and material sample temperature strongly influence the erosion rate. In this experiment, the particle velocity was controlled by varying the tunnel air flow rate. The particle impingement angle was set by rotating the sample relative to the flow stream direction. The erosion rate was determined from the relation: erosion rate=change in mass of sample/mass of impacting particles. The erosion testing for all samples was performed for same impact velocities at room temperature.

The variation of erosion rate with impingement angle is shown in Fig.6.

Firstly, the erosion rate vary from lowest to highest in an order of ZrAlN/Cu<ZrAlN<ZrN<Titanium alloy at each impingement angle from 15˚to 90˚ except ZrAlN somewhat higher than ZrN coating at 90˚. This is consistent with the hardness order of ZrAlN/Cu>ZrAlN>ZrN>Titanium alloy. Secondly, ZrAlN coating erosion rate increases with impingement angle, with maximum erosion rate at 90˚. While for titanium alloy, ZrN and ZrAlN/Cu coating erosion rate firstly incease then decreases with impingement angle. Titanium alloy shows maximum erosion rate at 30˚ impact angle, and has biggest erosion rate value. Coating ZrN exhibits maximum erosion at 45˚ particle impact angle, the erosion rate value is lower than that of titanium alloy. Coating ZrAlN/Cu shows maximum erosion rate at 45˚, but the erosion rate is lowest, indicating this coating has a long life and is very effective in protecting against erosion.

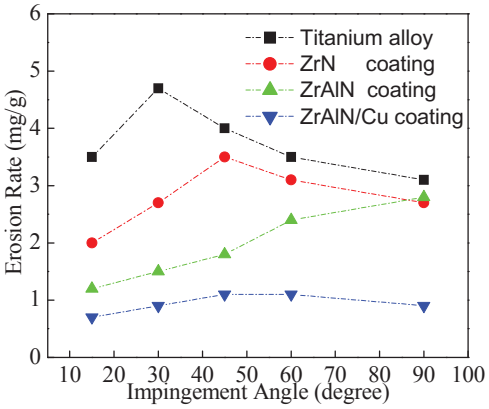

Fig.6 Erosion rate variation with impingement angle for titanium alloy, ZrN, ZrAlN and ZrAlN/Cu coating

For erosion damage, there are two dominant mechanism, i.e. the ductile-type damage through cutting and the brittle-type damage by cracking. For semi-brittle materials such as transition metal nitrides[8], cutting is the major erosion mechanism at a low impingement angle, while cracking plays a more significant role in erosion damage process at a high impingement angle. Given the different erosion damage mechanisms, it is widely perceived that coating hardness usually plays an important role in erosion resistance related to cutting, whereas coating toughness is critical for erosion resistance associated with cracking.

In this study, the relations between coating hardness and erosion rate for low-angle particle impact do follow a general trend, where higher coating hardness leads to lower erosion rate. The erosion rate of ZrAlN and ZrAlN/Cu coating at high impingement angle reveal that erosion-resistant performance depends not only on hardness, but also on the toughness of coating materials. For coating ZrAlN, its poor erosion resistance to high-angle(90˚) particle impact is simply caused by low toughness, even though the coating has a high hardness. Fig.7 is surface morphology of erosion-tested ZrAlN coating at 30˚and 90˚ attack angle; the severe cracking(90˚) indicates that this coating is much more brittle than its counterparts. For coating ZrAlN/Cu, it is the combination of good toughness and high hardness that give rise to the significantly improved erosion resistance. The mild erosion damage surface morphology of coating ZrAlN/Cu is shown in Fig.8.

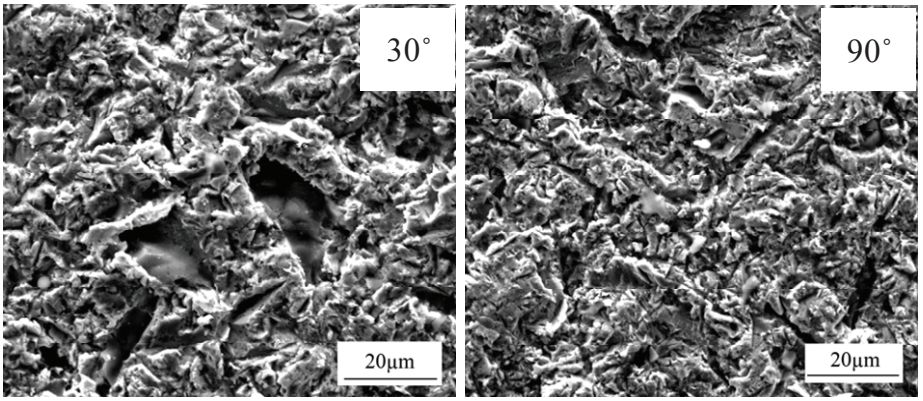

Fig.7 Surface morphology of erosion tested ZrAlN coating showing erosion damage by cutting and micro-cracking

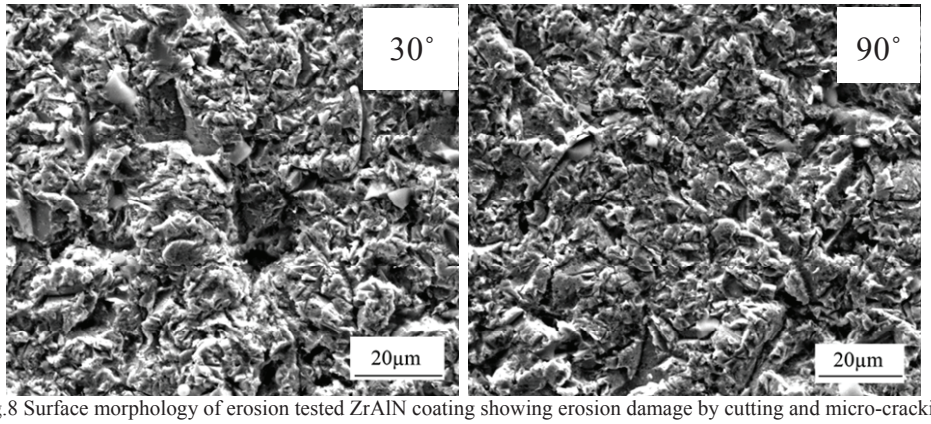

Fig.8 Surface morphology of erosion tested ZrAlN coating showing erosion damage by cutting and micro-cracking

4. Conclusions

In order to improve the erosion resistance of titanium alloy, high hardness and good toughness ZrAlN/Cu coating was deposited by Magnetron sputtering. ZrAlN/Cu coating containing 19%Al and 2%Cu (a.u.) was found possess a nano-columnar structure composed of ZrN columnar grains. Some of Al and Cu dissolved within ZrN grains; the coating is a mixture of ZrN, AlN and Cu nano-grains. 2%Cu does not decrease the hardness, ductile phase Cu overcomes the brittleness of ZrAlN coating, enhance coating toughness. ZrAlN/Cu exhibits the lowest erosion rates at all angles of incidence among all the coatings tested, it is clear that this coating provides best erosion resistance. The excellent erosion performance results from a good combination of high hardness and toughness.

Acknowledgments:

The authors acknowledge the support from National Key Laboratory for Remanufacturing Foundation. We are also grateful Ms Zhou for performing TEM analysis.

References

[1] N. Poondla, T.S. Srivatsan, A. Patnaik and M. Petraroli, J.Alloys Compd. 486 (2009)162
[2] M.W. Turner, M.J.J. Schmidt and L. Li. Appl. Surf. Sci. 247(2005)623
[3] A. Kermanpur, H. Sepehri Amin, S. Ziaei-Rad, N. Nourbakhshnia and M. Mosaddeghfar. Eng. Fail. Anal. 15(2008)1052
[4] V.A. Shulov, A.S. Novikov, A.G. Paikin and A.I. Ryabchikov.Surf. Coat. Technol. 201(2007)8105
[5] A. Neville, B.A.B. McDougall. Wear. 250(2001)726
[6] M. Ahmad, M. Casey and N. Sürken. Wear. 267(2009)1605
[7] Ani Zhecheva, Wei Sha, Savko Malinov and Adrian Long. Surf. Coat. Technol. 200(2005)2192
[8] Q. Yang, D.Y. Seo, L.R. Zhao and X.T.Zeng. Surf. Coat. Technol. 188-189(2004)168
[9] Y. Makino, M. Mori, S. Miyake, K. Saito and K. Asami. Surf. Coat. Technol. 193(2005)219
[10] M.Audronis, O. Jimenez, A. Leyland and A. Matthews. J. Phys. D:App. Phys. 42(2009)1
[11] J.H. Hsieh, P.C. Liu and C. Li. Surf. Coat. Technology. 202(2008)5530
[12] A.A. Volinsky, J.B. Vella and W.W. Gerberich. Thin Solid Films.429(2003)201
[13] B.R. Lawn, A.G. Evans and D.B.Marshall. J.Am. Ceram. Soc. 63(1980)574
[14] I Petrov, P.B. Barna, L. Hultman and J.E. Greene. J. Vac. Sci. Technol. A:Vac. Surf. Films. 21(2003)117
[15] T.Y Tsui, G.M. Pharr and W.C. Oliver. Mater. Res. Soc. Symp. Proc.383(1995)447
[16] M. Jirout, J. Musil. Surf. Coat. Technol.200(2006)6792
[17] S.H. Sheng, R. F. Zhang and S. Veprek. Acta Materialia.56(2008)968
[18] J. Musil, P. Zeman, H. Hruby and P.H. Mayrhofer. Suf. Coat. Technol.120-121(1999)179
[19] M. Audronis , O. Jimenez and A. Leyland .J.Phys.D:Appl.Phys. 42(2009)1
[20] S. Zhang, D. Sun, Y.Q. Fu and H.J. Du. Surf. Coat. Technol. 198(2005)74